

Supporting Information

Asymmetric deposition on high-speed moving superhydrophobic surfaces

Meng Wang,^a Youhua Jiang,^b Peng Gao,^c Ting Lu,^b Jiahua Lu,^a Tongfu Su,^a Shun Wang,^{*a} Hang Ding,^c
Zhichao Dong,^{*d} Meirong Song^{*a}

^aCollege of Science, Henan Agricultural University, Zhengzhou 450002, China

^bDepartment of Mechanical Engineering (Robotics), Guangdong Technion – Israel Institute of Technology, Shantou 515063, China

^cDepartment of Modern Mechanics, University of Science and Technology of China, Hefei 230022, China

^dCAS Key Laboratory of Bio-inspired Materials and Interfacial Science, Technical Institute of Physics and Chemistry, Chinese Academy of Sciences Future Technology College, University of Chinese Academy of Sciences, Chinese Academy of Sciences, Beijing 100190, China

*** E-mail address:**

Shun Wang: wangshun@henau.edu.cn

Zhichao Dong: dongzhichao@mail.ipc.ac.cn

Meirong Song: smr770505@henau.edu.cn

Supporting Information Includes:

One file with 8 Supporting Figures, 4 Supporting Tables, and 5 Video files as Supporting Movies.

Figure S1 — S8

Fig. S1. The shear viscosity and surface tension of aqueous droplet in Table S1.

Fig. S2. The dynamic surface tensions and shear viscosities for six droplets in Fig.1. (A) Dynamic surface tensions. (B) Shear viscosities.

Fig. S3. Time evolution of the centre of the spreading circle x_0 .

Fig. S4. (A) Time evolution of the visual downstream contact angle ($\theta_{V\text{down}}$). (B) Time evolution of the visual downstream contact point velocity ($V_{\text{VTCp(down)}}$).

Fig. S5. (A) Comparison of the ratio of viscosity to surface tension. (B) The relationship between $\cos\theta_d$ and Ca_d . Here, θ_d refers to $\theta_{V\text{up}}$.

Fig. S6. Shear viscosity versus the mass fraction of 1% AOT + ω % PEG or PEO.

Fig. S7. The difference between PEG and PEO in water. (A) Interaction network structure due to intermolecular hydrogen bonding between PEG and water molecules. (B) Extension effect due to intermolecular hydrogen bonding between PEO and water molecules. So, the PEG mainly increase the shear viscosity and PEO significantly improve the elongational viscosity.

Fig. S8. Critical linear velocity V for deposition on HM-SHB surface versus the impact velocity U .

Table S1 — S4

Table S1. Comparison of impact outcomes (impacting velocity U is 1.78 m s^{-1}) on static and moving SHB surfaces for droplets containing reported components.

Table S2. Parameters of six droplets in Fig.1

Table S3. Contact times for six droplets in Fig.1

Table S4. The shear viscosities and surface tensions for aqueous solutions of 1% AOT + ω % PEG or PEO

Movie S1 — S5

Movie S1. Comparison the impacts of reported components on static and moving superhydrophobic surface (impacting velocity is 1.78 m s^{-1})

Movie S2. Comparison of droplets impacting on static and moving superhydrophobic surface (Top view)

Movie S3. Comparison of droplets impacting on static and high-speed moving superhydrophobic surface (Side view)

Movie S4. The deposition failure of PEO additive with a molecular weight of 4,000,000

Movie S5. Deposition of water and the binary-additive AP droplets on different superhydrophobic surfaces

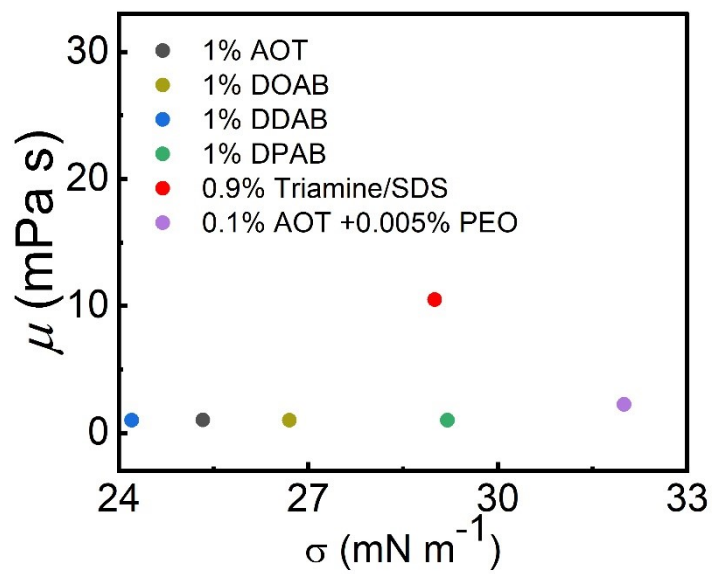


Fig. S1 The shear viscosity and surface tension of aqueous droplet in Table S1.

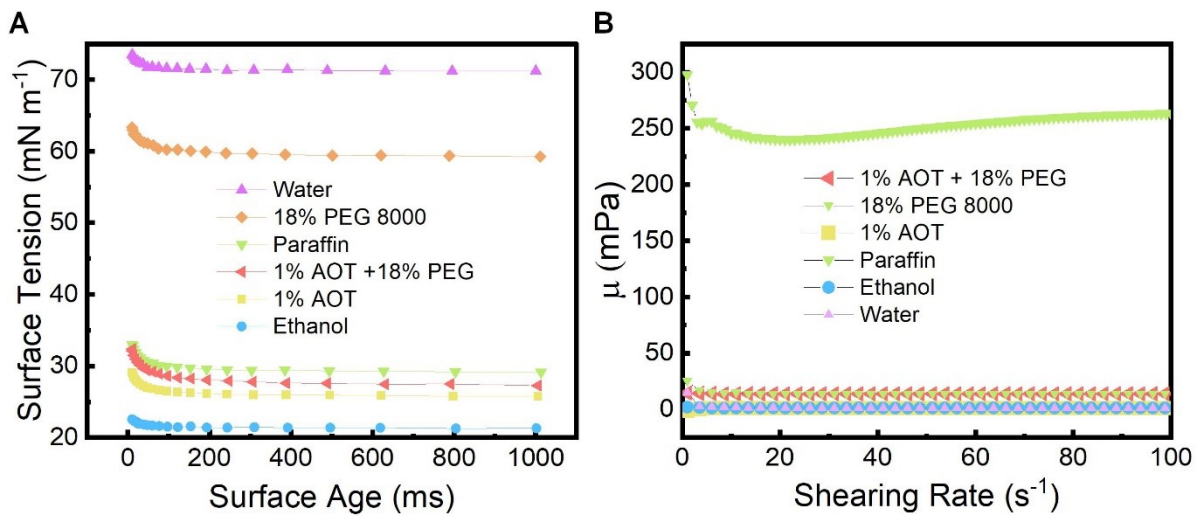


Fig. S2 The dynamic surface tensions and shear viscosities for six droplets in Fig. 1. (A) Dynamic surface tensions. (B) Shear viscosities.

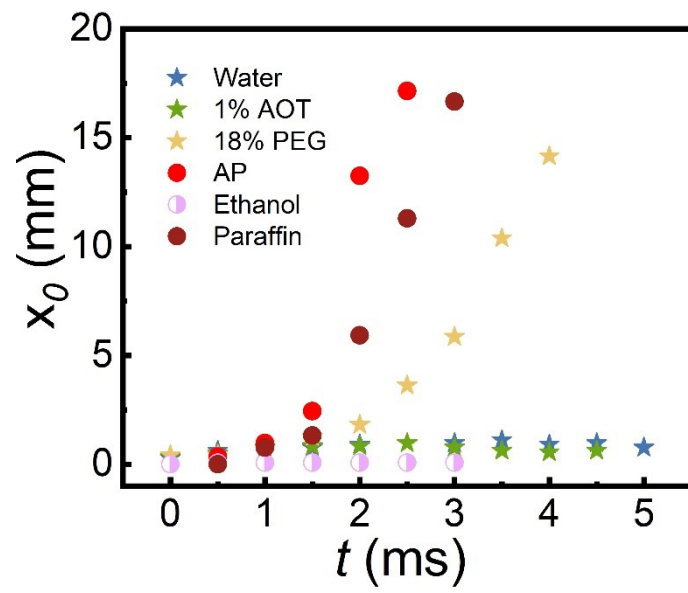


Fig. S3 Time evolution of the centre of the spreading circle x_0 .

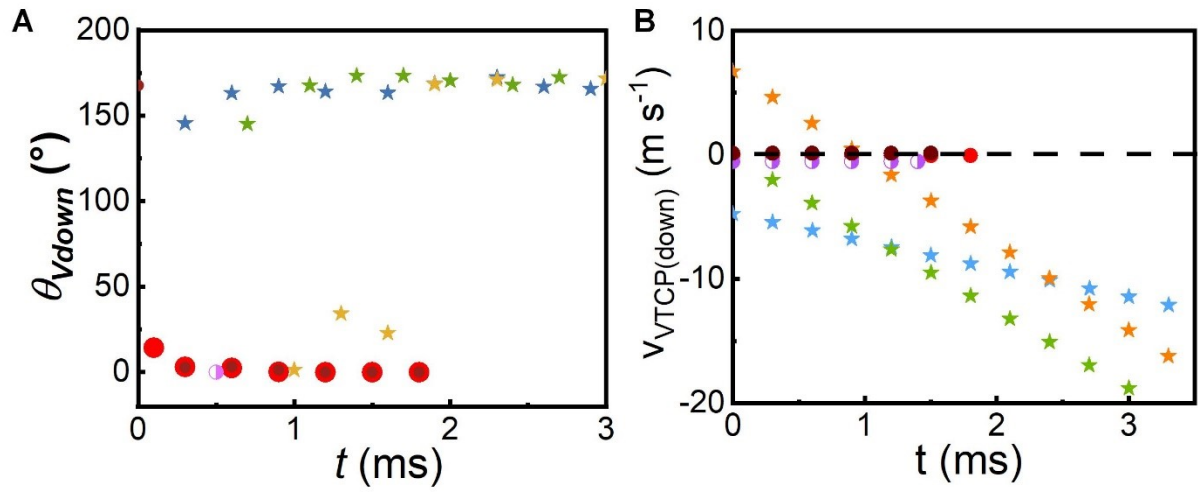


Fig. S4 (A) Time evolution of the visual downstream contact angle ($\theta_{V\text{down}}$). (B) Time evolution of the visual downstream contact point velocity ($V_{V\text{TCP}(\text{down})}$).

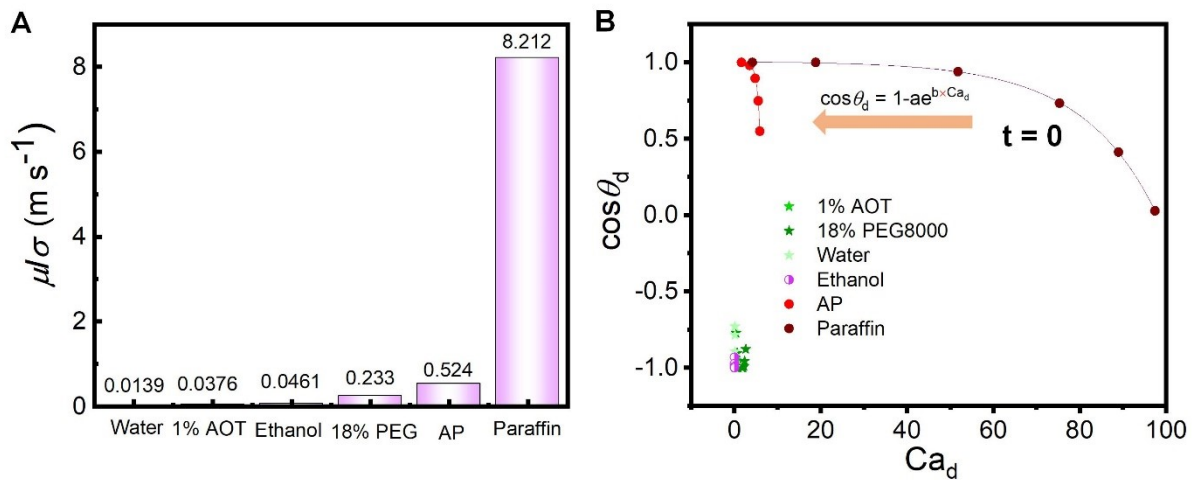


Fig. S5 (A) Comparison of the ratio of viscosity to surface tension. (B) The relationship between $\cos\theta_d$ and Ca_d . Here, θ_d refers to θ_{Vup} .

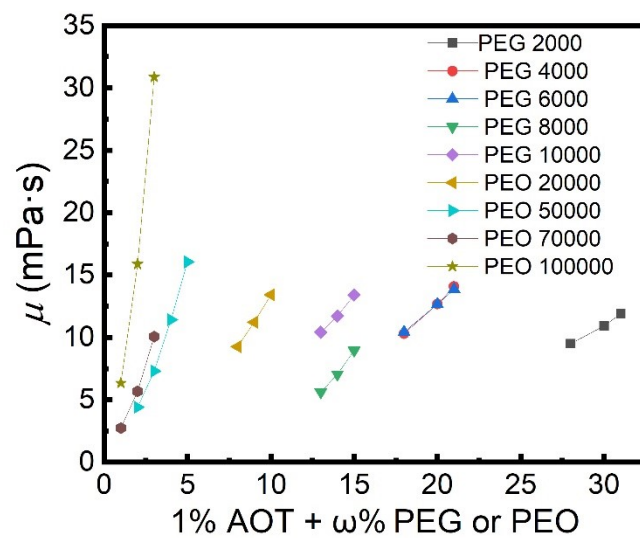


Fig. S6 Shear viscosity versus the mass fraction of 1% AOT + ω % PEG or PEO

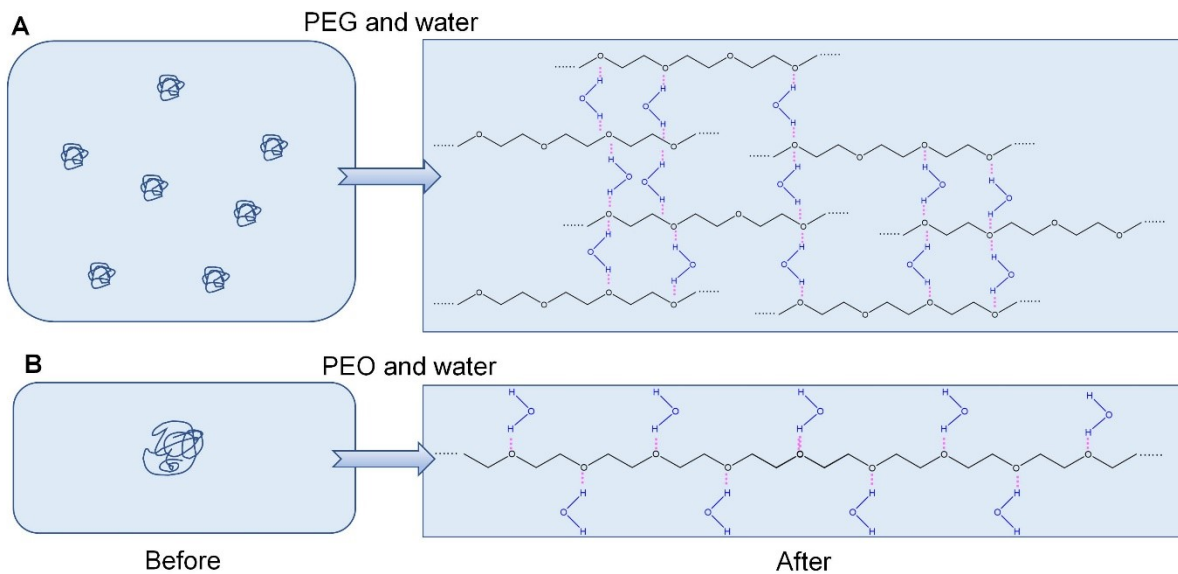


Fig. S7 The difference between PEG and PEO in water. (A) Interaction network structure due to intermolecular hydrogen bonding between PEG and water molecules. (B) Extension effect due to intermolecular hydrogen bonding between PEO and water molecules. So, PEG mainly increase the shear viscosity and PEO significantly improve the elongational viscosity.

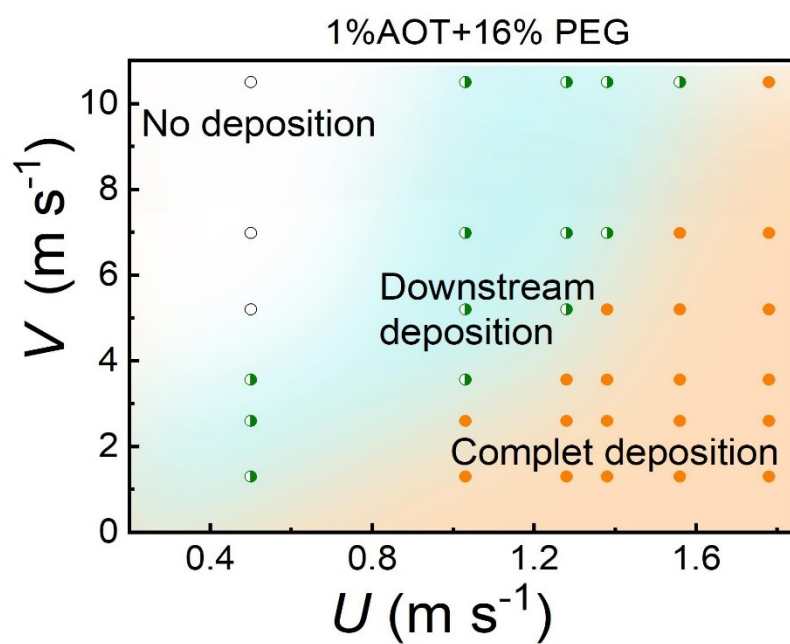


Fig. S8 Critical linear velocity V for deposition on HM-SHB surface versus the impact velocity U .

Table S1. Comparison of impact outcomes (impacting velocity U is 1.78 m s^{-1}) on static and moving SHB surfaces for droplets containing reported components.




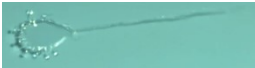

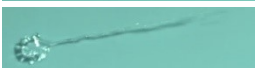

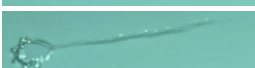


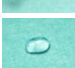

Component in aqueous droplet	Deposition on static SHB surface		Non-deposition on moving SHB surface ($V=10.5 \text{ m s}^{-1}$)		
1% AOT [1]	●		○		Flying balloons
0.9% Triamine/SDS [2]	●		○		
1% DOAB [3, 4]	●		○		
1% DDAB [3]	●		○		
1% DPAB [3]	●		○		
0.1% AOT + 0.005% PEO [5]	●		○		

Table S2. Parameters of six droplets in Fig. 1

Substance	ρ (kg m⁻³)	D_0 (mm)	V (m s⁻¹)	U (m s⁻¹)	Ca	We	Re
Water	996.60	2.30	10.5	1.78	0.15	101.99	24312.64
Ethanol	778.09	2.03	10.5	1.78	0.48	230.09	16579.23
1% AOT	997.98	1.71	10.5	1.78	0.39	213.00	18770.41
18% PEG 8000	1028.73	2.12	10.5	1.78	2.45	118.74	1687.79
Paraffin	826.77	2.25	10.5	1.78	86.23	201.42	81.28
1% AOT+18% PEG	1029.38	1.73	10.5	1.78	5.50	217.62	1375.86

Table S3. Contact times for six droplets in Fig.1

Substance	t_m (ms)	t_s (ms)	Reduction
Water	3.7	10.2	63.7%
Ethanol	3.6	∞	∞
1% AOT	3.7	∞	∞
18% PEG 8000	5.0	20.3	75.4%
Paraffin	∞	∞	0
1% AOT+18% PEG	∞	∞	0

Notes: t_s and t_m are the contact times for six droplets impacting on static and high-speed moving (HM) surfaces, respectively.

Table S4. The shear viscosities and surface tensions for aqueous solutions of 1% AOT + ω % PEG or PEO

Mv (PEG or PEO)	1% AOT + ω % PEG or PEO		
	ω (%)	μ (mPa s)	σ (mN m ⁻¹)
2000	28	9.50	27.44
	30	10.97	27.76
	31	11.89	27.80
4000	18	10.30	26.59
	20	12.66	26.77
	21	14.08	26.79
6000	18	10.43	26.22
	20	12.66	26.12
	21	13.85	26.23
8000	10	5.62	26.04
	12	7.04	25.86
	14	8.95	26.10
	16	11.37	25.84
	18	13.60	25.95
	20	17.97	25.90
10000	13	10.41	26.36
	14	11.71	26.35
	15	13.40	26.35
20000	8	9.25	25.95
	9	11.21	26.02
	10	13.41	26.36
50000	2	4.39	25.15
	3	7.30	25.08
	4	11.41	25.03
	5	16.05	25.01
70000	1	2.74	25.11
	2	5.67	25.05
	3	10.06	25.12
100000	1	6.34	25.35
	2	15.88	25.07
	3	30.89	25.11

References

- 1 M. Song, J. Ju, S. Luo, Y. Han, Z. Dong, Y. Wang, Z. Gu, L. Zhang, R. Hao and L. Jiang, *Sci. Adv.*, 2017, **3**, e1602188.
- 2 S. Luo, Z. Chen, Z. Dong, Y. Fan, Y. Chen, B. Liu, C. Yu, C. Li, H. Dai, H. Li, Y. Wang and L. Jiang, *Adv. Mater.*, 2019, **31**, 1904475.
- 3 H. Li, Z. Liu, C. Li, Q. Feng, Y. Liu, Q. Li, Z. Dong, Y. Wang and L. Jiang, *J. Mater. Chem. A*, 2020, **8**, 17392–17398.
- 4 H. Li, Z. Cai and Y. Wang, *Langmuir*, 2020, **36**, 14113–14122.
- 5 M. Song, D. Hu, X. Zheng, L. Wang, Z. Yu, W. An, R. Na, C. Li, N. Li, Z. Lu, Z. Dong, Y. Wang and L. Jiang, *ACS Nano*, 2019, **13**, 7966–7974.